



Carbon supported trimetallic PdNiAg nanoparticles as highly active, selective and reusable catalyst in the formic acid decomposition

Mehmet Yurderi^a, Ahmet Bulut^a, Mehmet Zahmakiran^{a,*}, Murat Kaya^b

^a Department of Chemistry, Science Faculty, Yüzüncü Yıl University, 65080 Van, Turkey

^b Department of Chemical Engineering and Applied Chemistry, Atilim University, 06836 Ankara, Turkey

ARTICLE INFO

Article history:

Received 20 April 2014

Received in revised form 20 May 2014

Accepted 6 June 2014

Available online 13 June 2014

Keywords:

Formic acid
Dehydrogenation
Nanoparticles
Palladium
Nickel
Silver
Alloy
Carbon

ABSTRACT

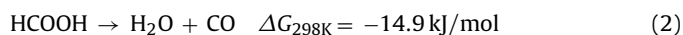
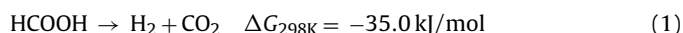
Trimetallic PdNiAg nanoparticles supported on activated carbon were simply and reproducibly prepared by wet-impregnation followed by simultaneous reduction method without using any stabilizer at room temperature. The characterization of the resulting material was done by the combination of complementary techniques and the sum of their results shows that the formation of well-dispersed 5.6 ± 2.2 nm PdNiAg nanoparticles in alloy form on the surface of activated carbon. These carbon supported PdNiAg nanoparticles were employed as heterogeneous catalyst in the catalytic decomposition of formic acid, which has great potential as a safe and convenient hydrogen carrier for fuel cells, under mild conditions. It was found that PdNiAg/C can catalyze the dehydrogenation of formic acid with high selectivity ($\sim 100\%$) and activity ($\text{TOF} = 85 \text{ h}^{-1}$) at 50°C . More importantly, the exceptional stability of PdNiAg nanoparticles against to agglomeration, leaching and CO poisoning make PdNiAg/C reusable catalyst in the formic acid dehydrogenation. PdNiAg/C catalyst retains almost its inherent activity ($>94\%$) even at 5th reuse in the dehydrogenation of formic acid with high selectivity ($\sim 100\%$) at complete conversion. The work reported here also includes the compilation of kinetic data for PdNiAg/C catalyzed dehydrogenation of formic acid depending on catalyst [PdNiAg], substrate [HCOOH], promoter [HCOONa] concentrations and temperature to determine the rate expression and the activation parameters (E_a , ΔH^\ddagger , and ΔS^\ddagger) of the catalytic reaction.

© 2014 Elsevier B.V. All rights reserved.

1. Introduction

Hydrogen has been considered as a clean energy carrier [1,2], since only water and small amounts of heat are the byproducts when it is utilized in proton exchange membrane fuel cells (PEMFC) [3,4]. Today, there have been serious efforts to achieve safe and efficient chemical hydrogen storage as it remains one of the most difficult problems in the transition from fossil fuels to hydrogen-based fuel cells energy technologies [1–4]. At this concern, formic acid (FA, HCOOH), which is one of the major products formed in biomass processing and also accessible via variety of processes such as hydrolysis of methyl formate or CO_2 hydrogenation [5,6], has been intensely investigated in the chemical hydrogen storage due to its high energy density, stability and nontoxicity [7,8]. In general, FA can be decomposed via dehydrogenation (1) and dehydration

(2) pathways depending on the catalyst, pH of the medium and the reaction temperature [7].



The dehydration of FA (2) is the unwelcome reaction and should be avoided for following conversion of hydrogen into electrical energy in PEMFC, as it produces CO impurity, which is highly toxic to fuel cell catalysts [9]. Recently, selective dehydrogenation of FA at remarkable hydrogen generation rates has been achieved by different homogeneous catalysts [10]. However, the problems in the separation and reusability of these homogeneous catalysts hinder their use in practical applications. In this connection, owing to the advantages of nanocatalysis [11], the current research has been directed toward the development of metal nanocatalysts (NCs) that can provide high activity, selectivity and stability in the dehydrogenation of FA [7]. Up to date, most of the attention on NCs toward FA dehydrogenation has been focused on noble metals [12–17] and among these catalysts Pd based NCs exhibit excellent catalytic performances in terms of activity and selectivity. Unfortunately, these

* Corresponding author. Tel.: +90 432 225 22 38; fax: +90 432 225 18 06.

E-mail addresses: mzahmakiran@gmail.com, zmehmet@yyu.edu.tr (M. Zahmakiran).

monometallic Pd NCs are easily deactivated throughout the catalytic decomposition of FA due to adsorption of poisonous carbon monoxide (CO) formed as intermediates. In this context, alloying with another metal that has better CO anti-poisoning ability over Pd, seems to be promising way to prevent CO-deactivation of Pd [18–23]. Alloying of Pd NPs with another metal especially first-row metals not only leads to the enhancement of the catalytic performance but also reduce the consumption of high-cost Pd. Therefore, it is highly fascinating to further increase CO resistance, catalytic performance of Pd NPs and lower the cost of nanocatalyst by integration of low-cost metals.

Herein, we report a facile synthesis of PdNiAg NPs supported on activated carbon, hereafter referred to as PdNiAg/C, and their excellent catalysis in the dehydrogenation of FA under mild conditions ($<90^{\circ}\text{C}$). PdNiAg/C were simply and reproducibly prepared through the conventional impregnation followed by simultaneous coupled plasma-optical emission spectroscopy (ICP-OES), powder X-ray diffraction (PXRD), X-ray photoelectron spectroscopy (XPS), conventional transmission electron microscopy (CTEM), high resolution transmission electron microscopy (HRTEM), scanning transmission electron microscopy (STEM), scanning transmission electron microscope-energy dispersive X-ray spectroscopy (STEM-EDX) and high angle annular dark field-scanning transmission electron microscopy (HAADF-STEM). The sum of their results revealed that the formation of well-dispersed 5.6 ± 2.2 nm PdNiAg NPs in the form of nanoalloy on the surface of activated carbon. The resulting PdNiAg NPs are acting as highly active ($\text{TOF} = 85 \text{ h}^{-1}$) and selective ($\sim 100\%$) heterogeneous catalyst in the dehydrogenation of FA at 50°C . Moreover, the exceptional durability of PdNiAg NPs even at high reaction temperature (70°C) against to agglomeration, leaching and CO poisoning make PdNiAg/C isolable, bottleable and highly reusable catalyst in the dehydrogenation of FA.

2. Experimental

2.1. Materials

Palladium(II) nitrate dihydrate ($\text{Pd}(\text{NO}_3)_2 \cdot 2\text{H}_2\text{O}$) ($\sim 40\%$ Pd basis), nickel(II) chloride hexahydrate ($\text{NiCl}_2 \cdot 6\text{H}_2\text{O}$), sodium borohydride (NaBH_4), sodium formate (CHO_2Na ; SF $\sim 98\%$), silver nitrate (AgNO_3 ; $\sim 99\%$) and activated carbon were purchased from Sigma-Aldrich®. Formic acid (CH_2O_2) was purchased from Merck® and all of them were used without further purification. Deionized water was distilled by water purification system (Milli-Q Water Purification System). All glassware and Teflon-coated magnetic stir bars were washed with acetone and copiously rinsed with distilled water before drying in an oven at 150°C .

2.2. Characterization

Pd, Ni and Ag contents of the samples were determined by ICP-OES (Leeman, Direct Reading Echelle) after each sample was completely dissolved in a mixture of HNO_3/HCl (1/3 ratio). Powder X-ray diffraction (XRD) patterns were recorded with a MAC Science MXP 3TZ diffractometer using $\text{Cu-K}\alpha$ radiation (wavelength 1.54 \AA , 40 kV , 55 mA). CTEM, HRTEM, STEM, and HAADF-STEM samples were prepared by dropping one drop of dilute suspension on copper coated carbon TEM grid and the solvent was then dried. The conventional TEM was carried out on a JEOL JEM-200CX transmission electron microscopes operating at 120 kV . HRTEM, STEM and HAADF-STEM were run on a JEOL JEM-2010F transmission electron microscope operating at 200 kV . Oxford EDXS system and Inca software were used to collect and process STEM-EDX data. HAADF-STEM images were acquired with a convergence angle of

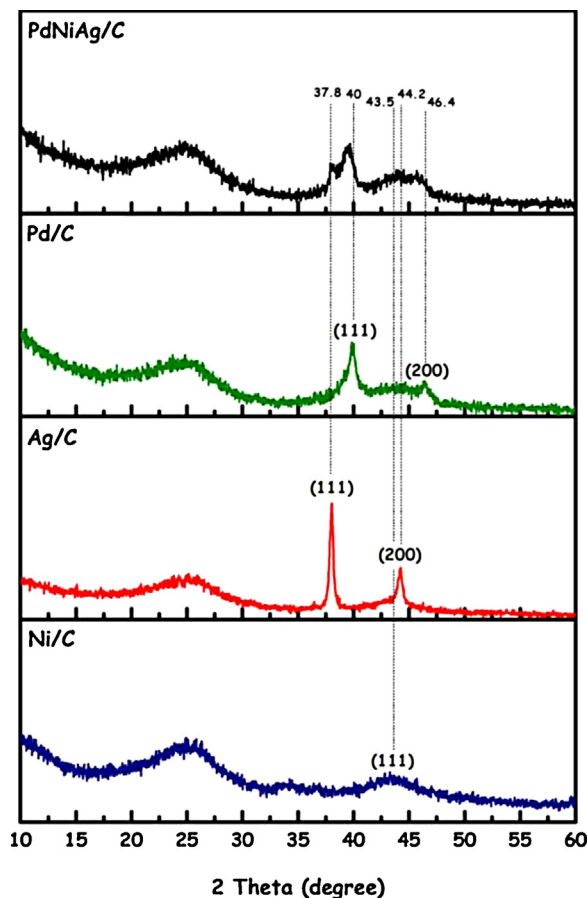


Fig. 1. P-XRD patterns of PdNiAg/C, Pd/C, Ag/C and Ni/C catalysts.

27 mrad and an inner collection angle of 100 mrad . EDX analysis was carried out with an electron beam size of 2 \AA . The XPS analyses were performed on a Physical Electronics 5800 spectrometer equipped with a hemispherical analyzer and using monochromatic $\text{Al-K}\alpha$ radiation (1486.6 eV , the X-ray tube working at 15 kV and 350 W , and pass energy of 23.5 eV). The gas generated from the decomposition of formic acid was analyzed by Shimadzu-GC-2014 analyzer.

2.3. Preparation of Pd/C, Ni/C and Ag/C catalysts

In a three separate experiments, 5.0 mL of $65.2 \text{ }\mu\text{mol}$ aqueous metal solution (Pd from $\text{Pd}(\text{NO}_3)_2 \cdot 2\text{H}_2\text{O}$; Ni from $\text{NiCl}_2 \cdot 6\text{H}_2\text{O}$, and Ag from AgNO_3) is mixed with activated carbon (140 mg) at 400 rpm for 2 h . Then, 1.0 mL aqueous solution of NaBH_4 (45.4 mg , 1.1 mmol) was added to this mixture and the resulting solution was stirred for half an hour under air at room temperature. After centrifugation (6000 rpm , 5 min), copious washing with water ($3 \times 20 \text{ mL}$), filtration, and drying in oven at 100°C , Pd/C, Ni/C and Ag/C catalysts were obtained as powder.

2.4. Preparation of PdAg/C, PdNi/C and NiAg/C catalysts

- (a) PdAg/C: 5.0 mL aqueous solution containing $\text{Pd}(\text{NO}_3)_2 \cdot 2\text{H}_2\text{O}$ (10.5 mg , $39.4 \text{ }\mu\text{mol}$ Pd), AgNO_3 (4.5 mg , $26.1 \text{ }\mu\text{mol}$ Ag) and activated carbon (140 mg) is mixed at 400 rpm for 2 h .
- (b) PdNi/C: 5.0 mL aqueous solution containing $\text{Pd}(\text{NO}_3)_2 \cdot 2\text{H}_2\text{O}$ (10.5 mg , $39.4 \text{ }\mu\text{mol}$ Pd), $\text{NiCl}_2 \cdot 6\text{H}_2\text{O}$ (6.0 mg , $25.4 \text{ }\mu\text{mol}$ Ni), and activated carbon (140 mg) is mixed at 400 rpm for 2 h .

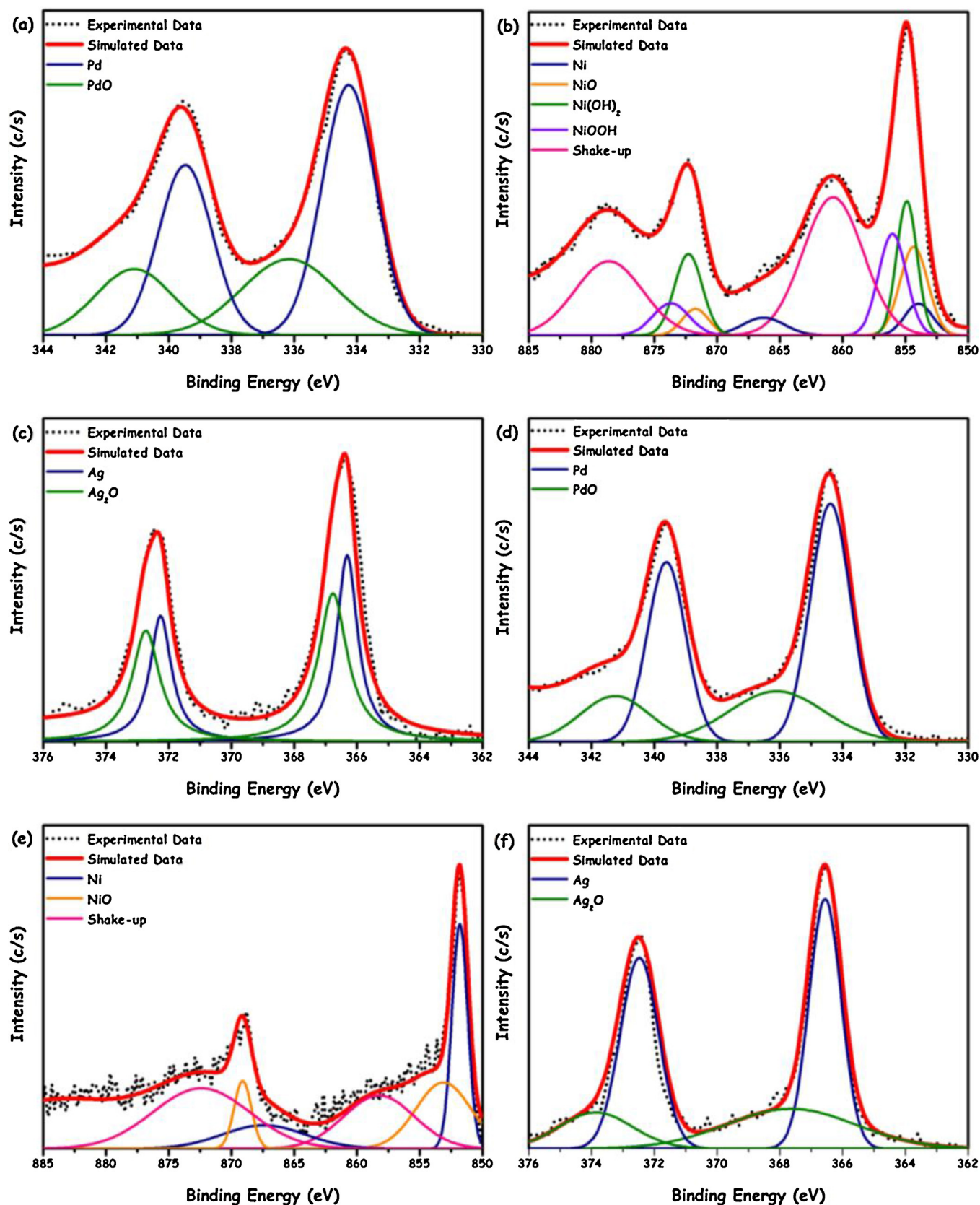


Fig. 2. High resolution (a) Pd 3d, (b) Ni 2p, (c) Ag 3d XPS spectra of PdNiAg/C; and high resolution (d) Pd 3d, (e) Ni 2p, (f) Ag 3d XPS spectra of PdNiAg/C after 5 min of Ar etching.

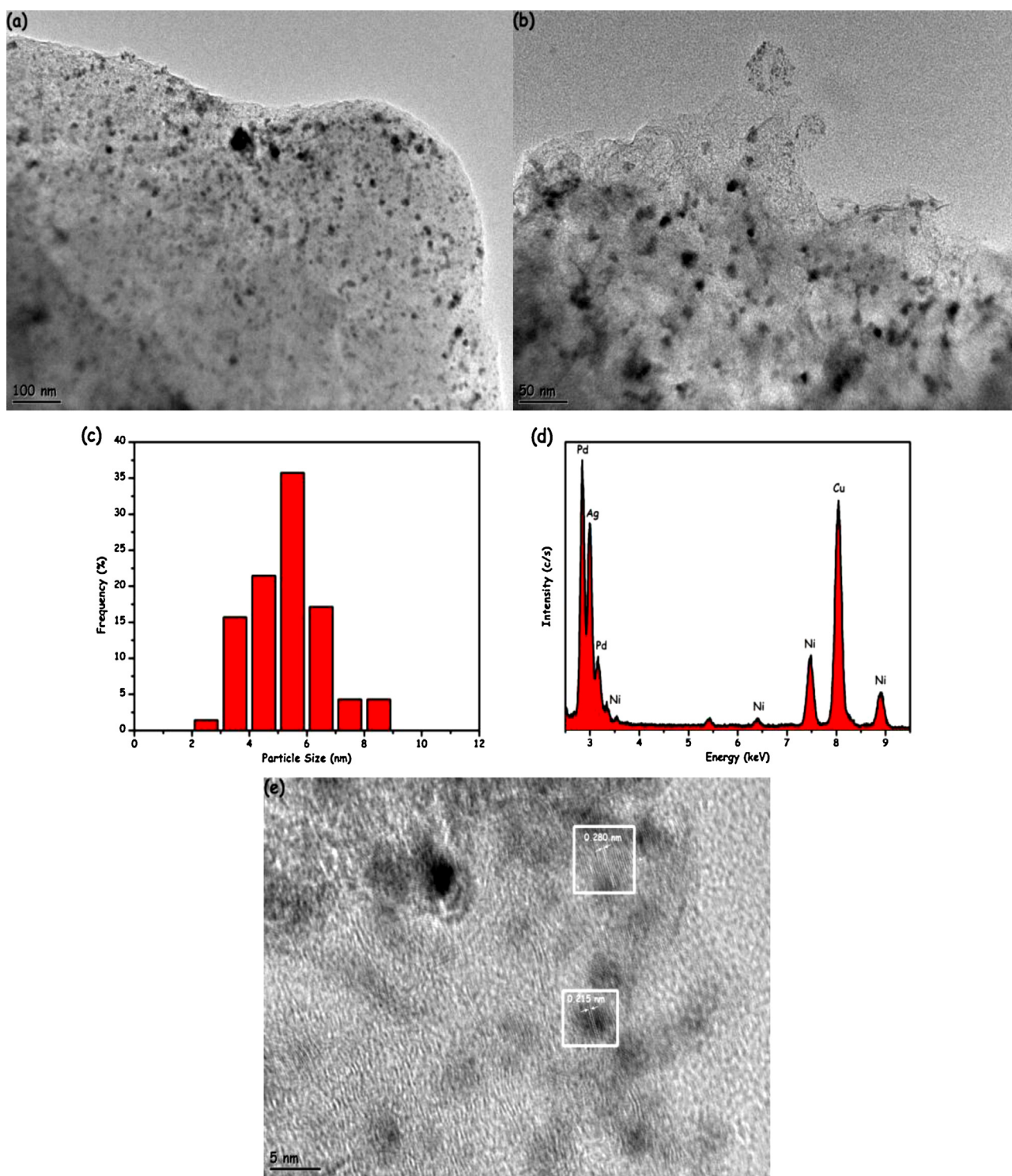


Fig. 3. (a)–(c) CTEM images of PdNiAg/C in different magnifications, (d) the size histogram of PdNiAg/C, (e) STEM-EDX spectrum of PdNiAg/C collected from the region given in (c), (f) and (g) HRTEM images of PdNiAg/C.

(c) AgNi/C: 5.0 mL aqueous solution containing AgNO_3 (5.6 mg, 32.5 μmol Ag), $\text{NiCl}_2 \cdot 6\text{H}_2\text{O}$ (7.5 mg, 31.9 μmol Ni), and activated carbon (140 mg) is mixed at 400 rpm for 2 h.

Then, into each separate mixtures 1.0 mL aqueous solution of NaBH_4 (45.4 mg, 1.1 mmol) was added and the resulting solutions were stirred for 30 min under ambient conditions. After centrifugation (6000 rpm, 5 min), copious washing with water (3×20 mL),

filtration, and drying in oven at 100 °C, PdAg/C, PdNi/C and NiAg/C catalysts were obtained as powder.

2.5. Preparation of PdNiAg/C catalyst

Typically, 5.0 mL aqueous solution containing $\text{Pd}(\text{NO}_3)_2 \cdot 2\text{H}_2\text{O}$ (10.5 mg, 39.4 μmol Pd), $\text{NiCl}_2 \cdot 6\text{H}_2\text{O}$ (3.0 mg, 12.7 μmol Ni), AgNO_3 (2.3 mg, 13.1 μmol Ag) and activated carbon (140 mg) is mixed at 400 rpm for 2 h. Then, 1.0 mL aqueous solution of

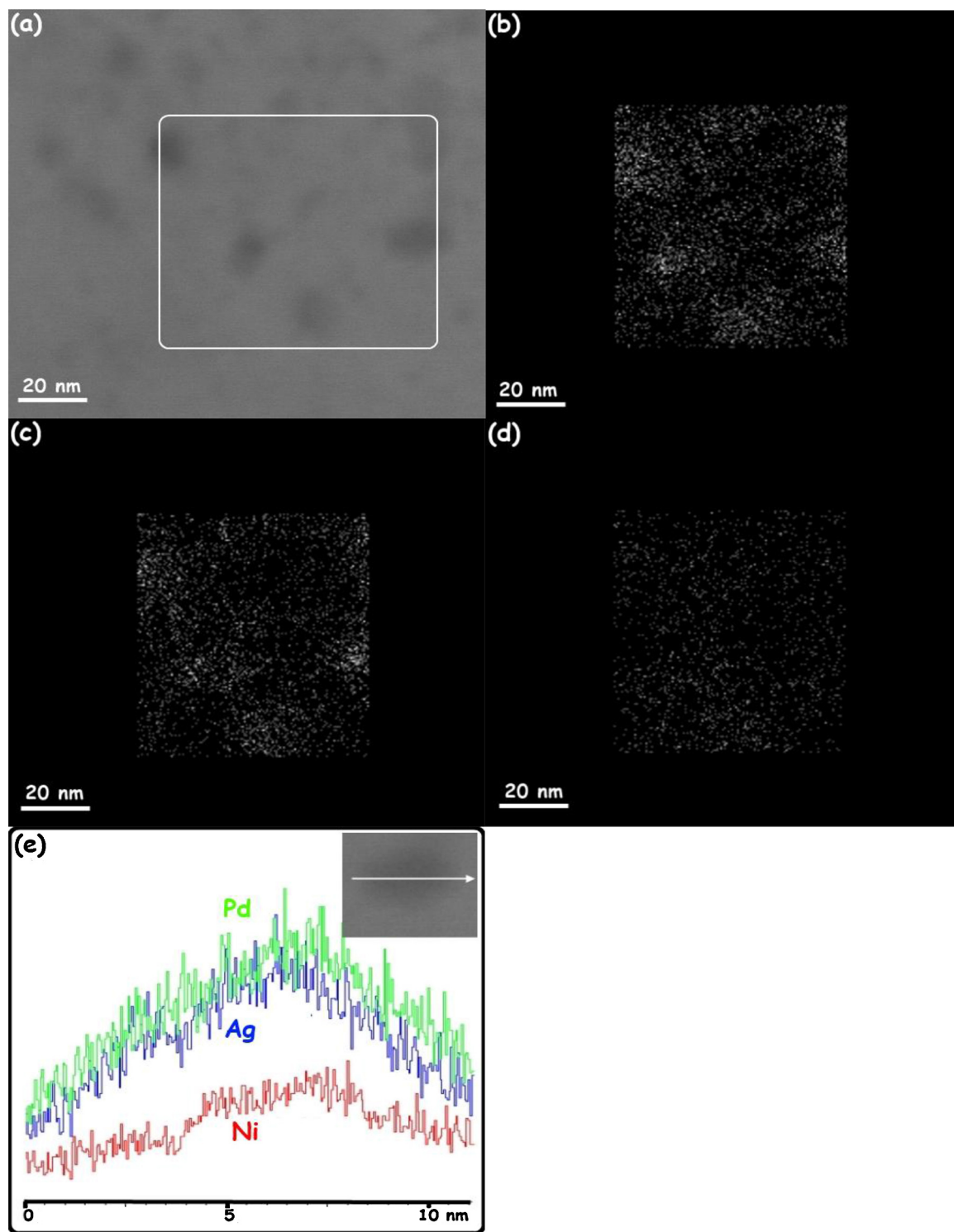


Fig. 4. (a) STEM image of PdNiAg/C, (b) STEM-Pd-mapping, (c) STEM-Ag-mapping, (d) STEM-Ni-mapping images of PdNiAg/C, (e) distribution of components in the PdNiAg NPs obtained by the line-scan analysis using STEM-EDX along the white arrow on the HAADFSTEM image of PdNiAg/C given in the inset.

NaBH_4 (45.4 mg, 1.1 mmol) was added to this mixture and the resulting solution was stirred for half an hour under air at room temperature. After centrifugation (6000 rpm, 5 min), copious washing with water (3×20 mL), filtration, and drying in oven at 100°C , PdNiAg/C catalyst was obtained as dark gray powder.

2.6. Determination of the catalytic activity of PdNiAg/C catalyst in the dehydrogenation of formic acid

The catalytic activity of PdNiAg/C in the dehydrogenation of FA was determined by measuring the rate of hydrogen generation. The volume of released gas during the reaction was monitored using

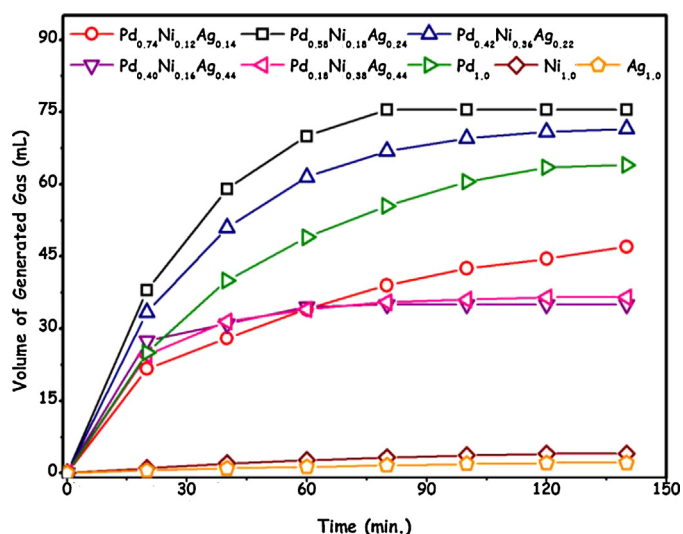


Fig. 5. The plot of the volume of the generated gas versus time for (a) monometallic ($\text{Pd}_{0.91}/\text{C}$, $\text{Ag}_{0.90}/\text{C}$, $\text{Ni}_{0.88}/\text{C}$), (b) bimetallic ($\text{Pd}_{0.55}\text{Ni}_{0.45}/\text{C}$, $\text{Pd}_{0.52}\text{Ag}_{0.48}/\text{C}$, $\text{Ni}_{0.58}\text{Ag}_{0.42}/\text{C}$), and (c) trimetallic ($\text{Pd}_{0.74}\text{Ni}_{0.12}\text{Ag}_{0.14}/\text{C}$, $\text{Pd}_{0.42}\text{Ni}_{0.36}\text{Ag}_{0.22}/\text{C}$, $\text{Pd}_{0.40}\text{Ni}_{0.16}\text{Ag}_{0.44}/\text{C}$, $\text{Pd}_{0.18}\text{Ni}_{0.38}\text{Ag}_{0.44}/\text{C}$) catalysts for the dehydrogenation of FA (in all [metal] = 2.85 mM, [FA] = [SF] = 0.175 M in 10.0 mL aqueous solution) at 50 °C.

the gas burette by water displacement. Before starting the catalytic activity test, a jacketed one necked reaction flask (50.0 mL) containing a Teflon-coated stir bar was placed on a magnetic stirrer (Heidolph MR-3004) and thermostated to 50 °C by using a constant temperature bath (Lab Companion RW-0525). In a typical experiment, PdNiAg/C catalyst was weighed and transferred into the reaction flask, and then 9.0 mL H_2O was added into the reaction flask and this mixture was stirred for 15 min to achieve thermal equilibrium. Next, 1.0 mL aqueous FA solution (0.175 M FA + 0.175 M SF) was added into the reaction flask via its septum by using a 1.0 mL gastight syringe and the catalytic reaction was started ($t=0$ min) by stirring the mixture at 600 rpm.

2.7. NaOH trap experiment

To determine CO_2 to H_2 molar ratio in the gas mixture generated during the PdNiAg/C catalyzed dehydrogenation of 10.0 mL aqueous FA solution (0.175 M FA + 0.175 M SF), NaOH trap experiment was performed as reported elsewhere [14–19]. In this experiment, the trap (10 M NaOH solution) was placed between the jacketed reactor and gas burette. The generated gas during the reaction was passed through the NaOH trap and the CO_2 was captured. Next, the volume of the gas generated from the dehydrogenation of FA was monitored and compared to those without trap experiment.

2.8. Isolability and reusability of PdNiAg/C catalyst in the dehydrogenation of formic acid

After the first run of catalytic dehydrogenation of aqueous FA solution starting with PdNiAg/C at 70 ± 0.1 °C, the catalyst was isolated from reaction solution by centrifugation and washed with excess water, then dried at 100 °C. The dried catalyst was weighted and used again in the catalytic dehydrogenation of 10 mL aqueous FA solution (0.175 M FA + 0.175 M SF) at 70 °C.

3. Results and discussion

3.1. Preparation and characterization of PdNiAg/C catalyst

PdNiAg/C catalyst was simply and reproducibly prepared by wet-impregnation followed by simultaneous reduction method [24]. Typically, an aqueous solution containing palladium(II) nitrate, nickel(II) chloride, silver(I) nitrate and activated carbon was mixed for 2 h. Then, fresh NaBH_4 as a reducing agent ($[\text{NaBH}_4]/[\text{metal}]$ ratio was kept at ~ 15 to ensure complete reduction of metal ions) was added to this mixture and the resulting solution was stirred for half an hour under air at room temperature. After centrifugation, copious washing with water, and drying in oven at 100 °C, PdNiAg/C catalyst was obtained as dark gray powder and characterized by ICP-OES, XRD, XPS, TEM, HRTEM, STEM, STEM-EDX and HAADF-STEM.

The molar composition of the as-prepared catalyst was found to be $\text{Pd}_{0.58}\text{Ni}_{0.18}\text{Ag}_{0.24}$ (1.62% wt Pd, 0.29% wt Ni, and 0.71% wt Ag loadings correspond to 23.2 μmol Pd, 7.2 μmol Ni and 9.6 μmol Ag) by ICP-OES. Fig. 1 depicts P-XRD patterns of as prepared PdNiAg/C sample in addition to those of Pd/C (2.4 wt% Pd), Ni/C (1.96 wt% Ni) and Ag/C (2.05 wt% Ag) samples. PdNiAg/C sample exhibits well-defined diffraction peaks in the position between the corresponding Pd ([111] at 40° and [200] at 46.4°) [18], Ag ([111] at 37.8° and [200] at 44.2°) [25], and Ni/C ([111] at 46.4°) [26] indicative of the formation of alloy structure [27].

In order to determine the chemical environment and oxidation state of palladium, nickel and silver atoms on PdNiAg/C, we performed XPS measurements at Pd 3d, Ni 2p and Ag 3d core levels. Fig. 2(a–c) shows the high resolution Pd 3d, Ni 2p and Ag 3d XPS spectra and their deconvolution, which reveal that the chemical states of Pd, Ni and Ag in the catalyst are Pd ($\text{Pd } 3d_{5/2}$ 334.2 eV; $\text{Pd } 3d_{3/2}$ 339.5 eV), PdO ($\text{Pd } 3d_{5/2}$ 336.2 eV; $\text{Pd } 3d_{3/2}$ 341.1 eV) [28], Ni ($\text{Ni } 2p_{3/2}$ 853.9 eV; $\text{Ni } 2p_{1/2}$ 866.4 eV), NiO ($\text{Ni } 2p_{3/2}$ 854.2 eV; $\text{Ni } 2p_{1/2}$ 871.7 eV), Ni(OH)_2 ($\text{Ni } 2p_{3/2}$ 854.2 eV; $\text{Ni } 2p_{1/2}$ 871.7 eV) NiOOH ($\text{Ni } 2p_{3/2}$ 856 eV; $\text{Ni } 2p_{1/2}$ 873.7 eV) [29] and those of Ag are Ag ($\text{Ag } 3d_{5/2}$ 366.3 eV; $\text{Ag } 3d_{3/2}$ 372.2 eV), Ag_2O ($\text{Ag } 3d_{5/2}$ 366.8 eV; $\text{Ag } 3d_{3/2}$ 372.7 eV) [30]. The observation of oxide signals can be attributed to the surface oxidation of Pd, Ni and Ag NPs during XPS sampling procedure [31]. Expectedly, after Ar sputtering for only 5 min, most of the oxide states were removed and metallic Pd, Ni and Ag became the main states (Fig. 2(d–f)).

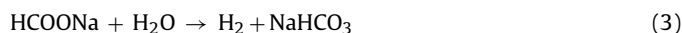
The size, morphology and composition of PdNiAg/C were investigated by CTEM, HRTEM, STEM, STEM-EDX, and HAADF-STEM. CTEM images of PdNiAg/C in different magnifications are given in Fig. 3(a–c), which show the presence of well-dispersed PdNiAg NPs in the range of 2.5–8.4 nm (mean: 5.6 ± 2.2 nm) and large size particles ~ 10 nm resulting from clumping of surface bound small particles (Fig. 3(d)). STEM-EDX spectrum of PdNiAg/C (Fig. 3(e)) collected from the region given in Fig. 3(c) confirms the presence of Pd, Ni and Ag in the analyzed region. HRTEM image of PdNiAg/C given in Fig. 3(f) and (g) reveal that crystalline nature of PdNiAg and the lattice fringes were measured to be 0.215 and 0.280 nm, which differ from (111) spacing of Pd (0.223 nm) [18], Ni (0.203 nm) [32], Ag (0.235 nm) [33] and (200) spacing of Pd (0.194 nm) [34], Ag (0.220 nm) [35].

The compositional survey of PdNiAg/C was done by STEM-EDX-mapping and HAADF-STEM techniques. Fig. 4(a–d) gives STEM and STEM-elemental mapping (for Pd, Ni and Ag) images of PdNiAg/C. Closer inspection of STEM-elemental mapping images (Fig. 4(b–d)) collected from the labeled region given in Fig. 4(a) shows that Pd, Ag and Ni atoms are distributed uniformly over the entire NPs. In addition to STEM-elemental mapping, we also performed HAADF-STEM line analyses, in which a minimum 10 individual NPs were compositionally analyzed, and the compositional distribution within each NP was found to be consistent. HAADF-STEM image of PdNiAg/C

given in the inset of Fig. 4(e) does not show any darker and brighter regions that can be assigned to the formation of core/shell structure [36–38]. Moreover, when the distribution of the elements in the chosen PdNiAg NPs was assessed by using the line scanning analysis in the STEM-EDX mode (Fig. 4(e)), we saw obviously overlapping of Pd, Ni and Ag signals. The results collected from P-XRD, HRTEM, STEM-mapping, and HAADF-STEM-line analyses are showing that PdNiAg NPs exist in alloy form on the surface of activated carbon.

3.2. Catalytic performance of PdNiAg/C in the dehydrogenation of formic acid

In general, sodium formate (HCOONa ; SF) as sodium salt of formic acid is added to catalytic dehydrogenation of FA to promote the activity of catalyst [14–16,39–42]. Recently, it has been reported that some homogeneous [43] and heterogeneous [28] catalysts can liberate H_2 through a catalytic hydrolysis of SF [28,43] (3).



For this reason we first performed a control experiment to check whether PdNiAg/C catalyzes the hydrolysis of SF, which was used in this study to promote the activity of PdNiAg/C in the catalytic dehydrogenation of FA. The result of this experiment showed that PdNiAg/C catalyzed hydrolysis of SF only produces 3.5 mL hydrogen gas over 2.5 h even at 70 °C. Although PdNiAg/C catalyzed hydrolysis of SF generates negligible amount of H_2 , all of

the catalytic activity results for PdNiAg/C catalyzed dehydrogenation of FA given here were corrected by subtracting the hydrogen gas generated from the hydrolysis of SF under identical conditions. As the next, the catalytic activities of $\text{Pd}_{0.58}\text{Ni}_{0.18}\text{Ag}_{0.24}/\text{C}$ together with its monometallic ($\text{Pd}_{0.91}/\text{C}$, $\text{Ag}_{0.90}/\text{C}$, $\text{Ni}_{0.88}/\text{C}$), bimetallic ($\text{Pd}_{0.55}\text{Ni}_{0.45}/\text{C}$, $\text{Pd}_{0.52}\text{Ag}_{0.48}/\text{C}$, $\text{Ni}_{0.58}\text{Ag}_{0.42}/\text{C}$), trimetallic ($\text{Pd}_{0.74}\text{Ni}_{0.12}\text{Ag}_{0.14}/\text{C}$, $\text{Pd}_{0.42}\text{Ni}_{0.36}\text{Ag}_{0.22}/\text{C}$, $\text{Pd}_{0.40}\text{Ni}_{0.16}\text{Ag}_{0.44}/\text{C}$, $\text{Pd}_{0.18}\text{Ni}_{0.38}\text{Ag}_{0.44}/\text{C}$) counterparts (in equimolar total metal concentrations) were investigated the dehydrogenation of FA at 50 °C and their results are presented in Fig. 5 (a–c). Obviously, $\text{Pd}_{0.58}\text{Ni}_{0.18}\text{Ag}_{0.24}/\text{C}$ catalyst provides a better activity than those of mono and bimetallic catalysts prepared by the same method. From Fig. 5 (a) and (b), it is clear that Pd is the crucial active metal in all catalysts; without Pd addition $\text{Ag}_{0.90}/\text{C}$, $\text{Ni}_{0.88}/\text{C}$, and $\text{Ni}_{0.58}\text{Ag}_{0.42}/\text{C}$ catalysts show no activity. Conversely, the initial activity of monometallic Pd ($\text{Pd}_{0.91}/\text{C}$) cannot resume as the active sites are easily deactivated by poisonous CO intermediate, which is one of the well-known important issues for the application monometallic catalysts in FA dehydrogenation [7,8].

Although, $\text{Pd}_{0.91}/\text{C}$ catalyst shows better activities than $\text{Pd}_{0.55}\text{Ni}_{0.45}/\text{C}$ and $\text{Pd}_{0.52}\text{Ag}_{0.48}/\text{C}$, its performance is still far from the trimetallic $\text{Pd}_{0.58}\text{Ni}_{0.18}\text{Ag}_{0.24}/\text{C}$. CTEM analyses of mono- and bimetallic catalysts (Figs. S1 and S2) showed that they have same shape but smaller size with respect to trimetallic $\text{Pd}_{0.58}\text{Ni}_{0.18}\text{Ag}_{0.24}$ NPs. Under these circumstances, the enhanced activity of $\text{Pd}_{0.58}\text{Ni}_{0.18}\text{Ag}_{0.24}/\text{C}$ catalyst can be explained by its special composition. The enhancement of Pd activity in FA dehydrogenation through

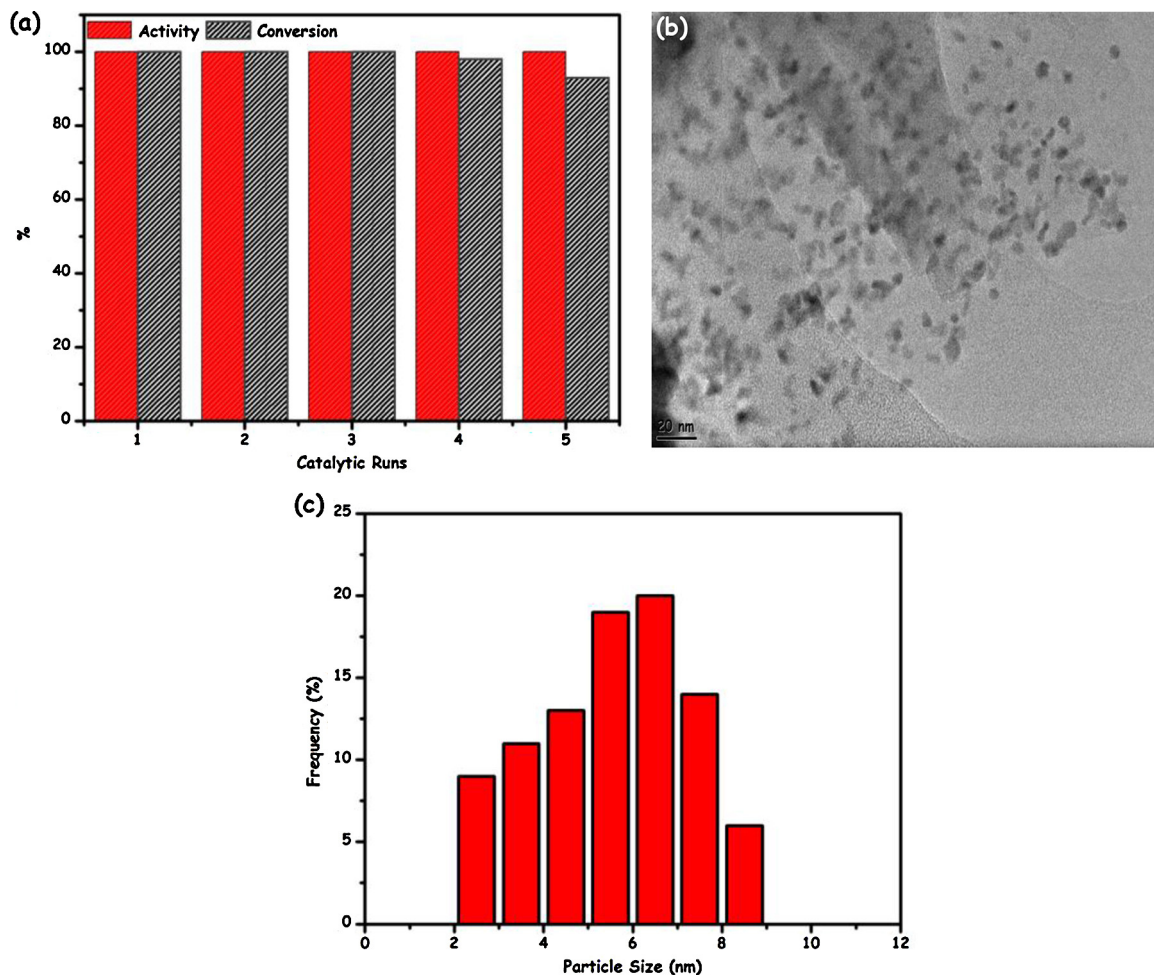


Fig. 6. (a) The percentage of conversion and retained catalytic activity of $\text{Pd}_{0.58}\text{Ni}_{0.18}\text{Ag}_{0.24}/\text{C}$ in the successive catalytic runs for the dehydrogenation of FA ($[\text{FA}] = [\text{SF}] = 0.175 \text{ M}$ in 10.0 mL aqueous solution) at 70 °C, (b) CTEM image and (c) corresponding size histogram of $\text{Pd}_{0.58}\text{Ni}_{0.18}\text{Ag}_{0.24}/\text{C}$ catalyst harvested after the fifth run of dehydrogenation of FA.

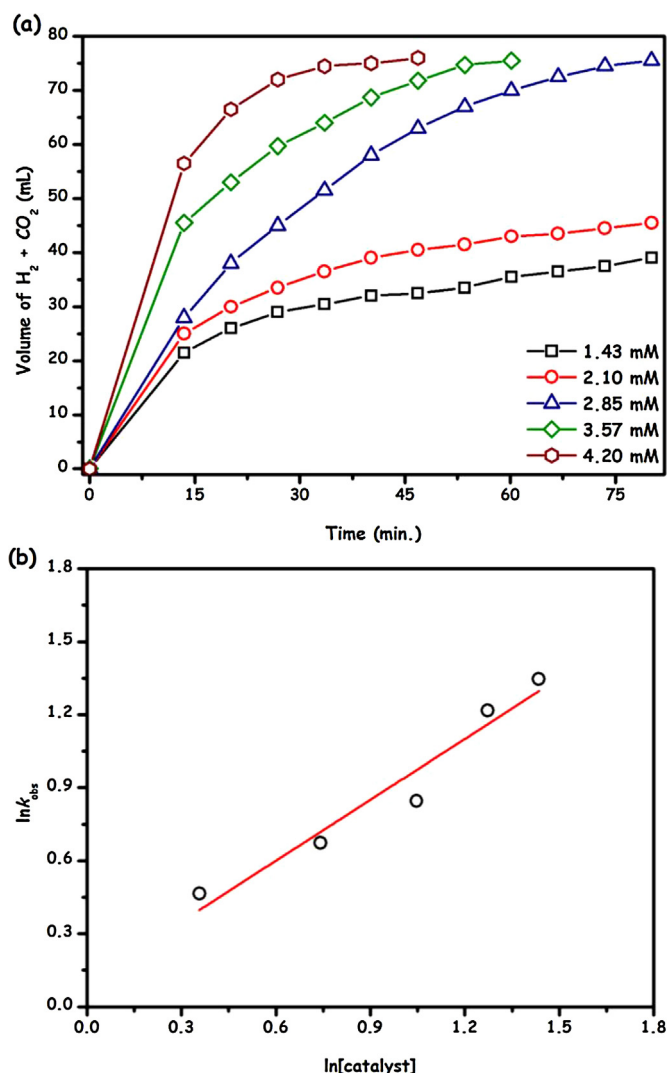


Fig. 7. (a) The volume of the generated gas (CO₂ + H₂) versus time graph, (b) plot of the hydrogen-generation rate versus the catalyst concentration (both in logarithmic scale; $y = 0.10 + 0.94x$ and $R^2 = 0.97$) for the dehydrogenation of FA ([FA] = [SF] = 0.175 M in 10.0 mL aqueous solution) starting with different Pd_{0.58}Ni_{0.18}Ag_{0.24}/C concentrations at 50 °C.

Ag and Ni incorporations has already been reported for AgPd [19], Ag@Pd [22], and PdNi@Pd [44] catalysts, which has been attributed to change in the electronic density (synergic effect) of Pd resulting from the formation of alloy and core-shell structures [19,22,44]. In our case alloying Pd, Ni, and Ag provides this synergistic effect on their catalysis and Pd_{0.58}Ni_{0.18}Ag_{0.24}/C is the optimum catalyst (Fig. 5(c)) that provides the best catalytic performance in terms of conversion and activity in the dehydrogenation of FA.

The generated gas over Pd_{0.58}Ni_{0.18}Ag_{0.24}/C was identified by gas chromatography (GC) and NaOH trap experiment [14,16], since dehydrogenation of FA is generally associated with the dehydration at relatively high reaction temperatures [7]. We found that the generated gas from Pd_{0.58}Ni_{0.18}Ag_{0.24}/C catalyzed dehydrogenation of FA is a mixture of H₂ and CO₂ with a 1.01:0.99 H₂:CO₂ molar ratio and no CO was detected (DL for CO ~10 ppm). This result reveals that CO-free H₂ generation can be achieved from aqueous FA solution by Pd_{0.58}Ni_{0.18}Ag_{0.24}/C, which is very important for fuel cell applications [9]. The turnover frequency (TOF) value of Pd_{0.58}Ni_{0.18}Ag_{0.24}/C was found to be 85 mol H₂ mol catalyst⁻¹ h⁻¹ at 50 °C, which is higher than the previously reported Au-Pd/ED-MIL-101 (49 mol H₂ mol catalyst⁻¹ h⁻¹ at 90 °C) [14], Pd@SiO₂

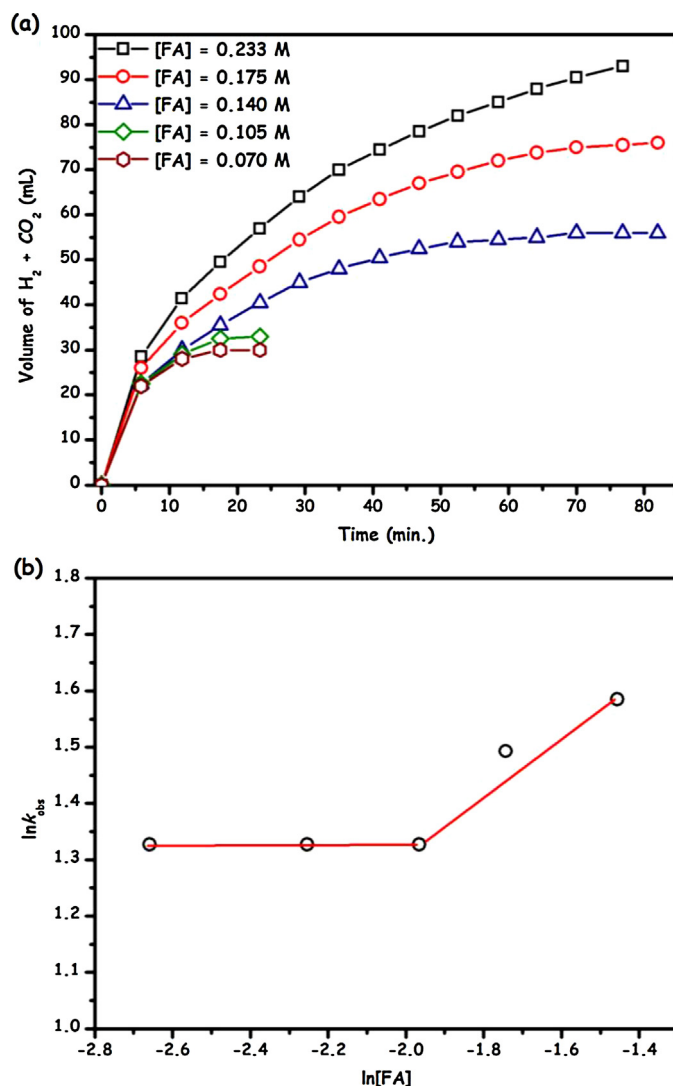


Fig. 8. (a) The volume of the generated gas (CO₂ + H₂) versus time graph, (b) plot of the hydrogen-generation rate versus the FA concentration (both in logarithmic scale) for Pd_{0.58}Ni_{0.18}Ag_{0.24}/C catalyzed dehydrogenation of FA ([catalyst] = 2.85 mM, [SF] = 0.175 M in 10.0 mL aqueous solution) starting with various FA concentrations at 50 °C.

(70 mol H₂ mol catalyst⁻¹ h⁻¹ at 90 °C) [16], Au/Al₂O₃ (64 mol H₂ mol catalyst⁻¹ h⁻¹ at 50 °C), Pd-Au/C (27 mol H₂ mol catalyst⁻¹ h⁻¹ at 92 °C) [39] and PdAu@Au/C (45 mol H₂ mol catalyst⁻¹ h⁻¹ at 92 °C) NPs [40] but still lower than PdNi@Pd/GNs-CB (66 mol H₂ mol catalyst⁻¹ h⁻¹ at 25 °C) [44] Pd@MSC-30 (2623 mol H₂ mol catalyst⁻¹ h⁻¹ at 50 °C) [45] tested in the dehydrogenation of FA by using SF as a promoter.

Apart from activity and selectivity, the reusability of Pd_{0.58}Ni_{0.18}Ag_{0.24}/C, as another crucial measures in heterogeneous catalysis, was also examined in the dehydrogenation of FA. When isolated and dried sample of Pd_{0.58}Ni_{0.18}Ag_{0.24}/C is reused in FA dehydrogenation, Pd_{0.58}Ni_{0.18}Ag_{0.24} NPs are still acting as active catalyst, as given in Fig. 6(a) they retain almost their inherent catalytic activity (>94%) even at the fifth catalytic run, with high selectivity (>99%) at almost complete conversion (≥90%). The slight decrease (~5%) observed in the activity of Ni_{0.18}Ag_{0.24} NPs in the fifth catalytic run may be attributed to the decrease in the number of active surface atoms due to the clumping of Pd_{0.58}Ni_{0.18}Ag_{0.24} NPs.

Indeed, a CTEM image of Pd_{0.58}Ni_{0.18}Ag_{0.24}/C (Fig. 6(b)) sample harvested after the fifth run of dehydrogenation of FA shows

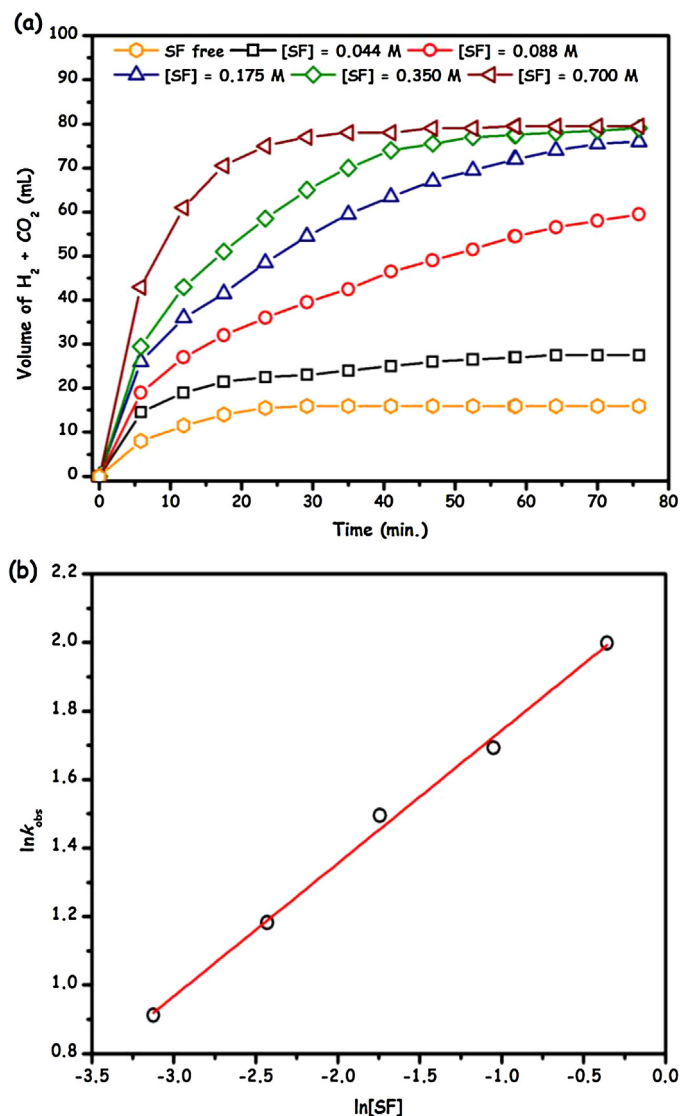


Fig. 9. (a) The volume of the generated gas (CO₂ + H₂) versus time graph, (b) plot of the hydrogen-generation rate versus the FA concentration (both in logarithmic scale; $y = 2.14 + 0.49x$ and $R^2 = 0.99$) for Pd_{0.58}Ni_{0.18}Ag_{0.24}/C catalyzed dehydrogenation of FA ([catalyst] = 2.85 mM, [FA] = 0.175 M in 10.0 mL aqueous solution) started with various SF concentrations at 50 °C.

an increase of the average size from 5.6 ± 2.2 nm to 5.9 ± 2.7 nm (Fig. 6(c)). ICP-OES analyses of recovered catalyst and reaction solutions gave us almost the identical metal amounts with that of the fresh catalyst and no leaching of metals (DL: 0.003 ppb for Ag, 0.2 ppb for Ni, 0.001 ppb for Pd) into the solution, respectively. Additionally, FA dehydrogenation was completely stopped by the removal of Pd_{0.58}Ni_{0.18}Ag_{0.24}/C from the reaction solution, which confirms that the retention of active Pd_{0.58}Ni_{0.18}Ag_{0.24} NPs on the support and no leaching of them to the solution. These results are indicative of the high stability of carbon supported Pd_{0.58}Ni_{0.18}Ag_{0.24} NPs against to agglomeration and leaching, which explain their exceptional reusability performance in the FA dehydrogenation.

3.3. Initial kinetic studies and determination of activation parameters for Pd_{0.58}Ni_{0.18}Ag_{0.24}/C catalyzed dehydrogenation of formic acid

Fig. 7(a) shows the plot of the volume of generated gas (CO₂ + H₂) versus the reaction time for the dehydrogenation of FA started with

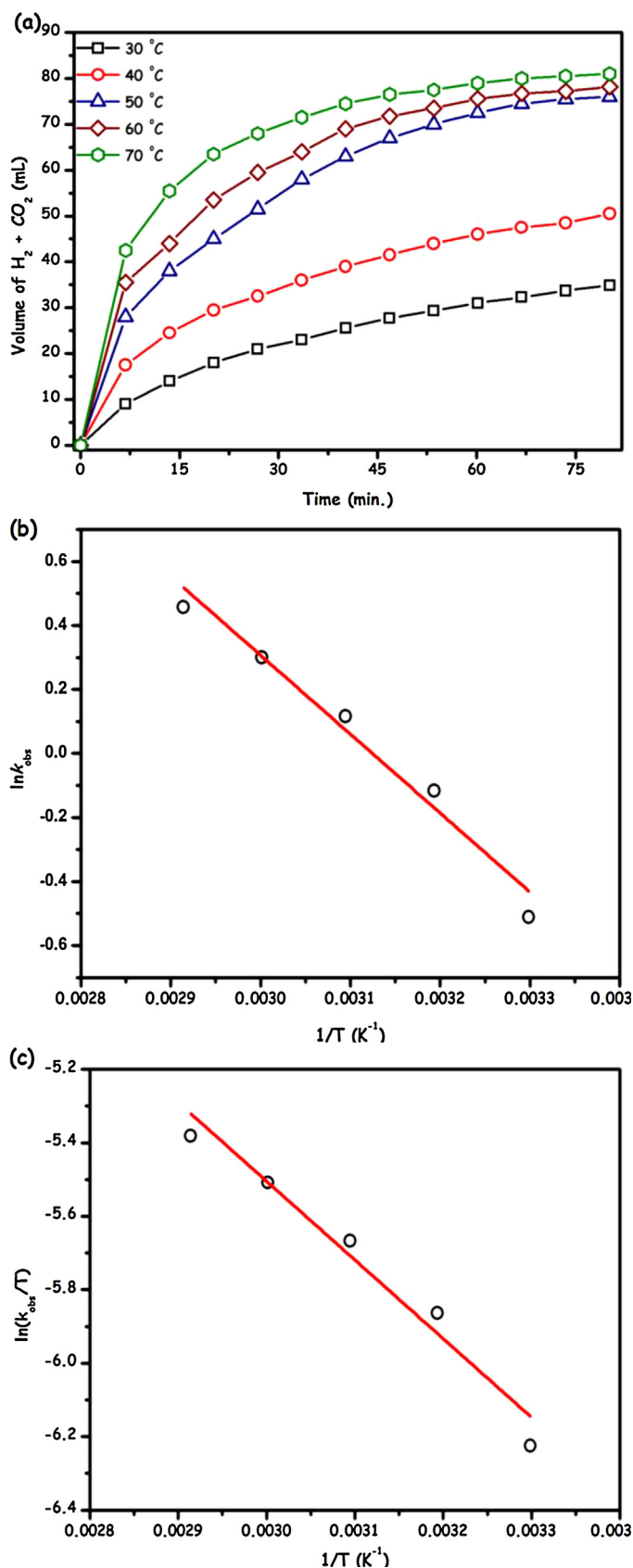


Fig. 10. (a) The volume of the generated gas (CO₂ + H₂) versus time graph, (b) Arrhenius plot ($y = 7.706 - 2466x$ and $R^2 = 0.98$) and (c) Eyring plot ($y = 0.925 - 2143x$ and $R^2 = 0.97$) for Pd_{0.58}Ni_{0.18}Ag_{0.24}/C catalyzed dehydrogenation of FA ([catalyst] = 2.85 mM, [FA] = [SF] = 0.175 M in 10.0 mL aqueous solution) at different temperatures.

different Pd_{0.58}Ni_{0.18}Ag_{0.24}/C concentrations at 50 °C. It should be noted that, the complete conversion of FA is achieved by using % 1.6 mol catalyst within one hour at 50 °C. The reaction rates for each catalyst concentration were calculated from the linear portion of each plots comprising reaction duration of 15 min. The logarithmic plot of the hydrogen generation rate versus catalyst concentration gives the line with a slope of 0.94 (Fig. 7(b)), which indicates that the reaction is close to first-order with respect to the catalyst concentration.

The effect of FA concentration on the rate of Pd_{0.58}Ni_{0.18}Ag_{0.24}/C catalyzed dehydrogenation of FA was studied by performing a series of experiments starting with the variation of the initial concentration of FA while keeping Pd_{0.58}Ni_{0.18}Ag_{0.24}/C and SF concentrations constant at 50 °C. Fig. 8(a) gives the graph of the volume of generated gas (CO₂ + H₂) versus the reaction time for Pd_{0.58}Ni_{0.18}Ag_{0.24}/C catalyzed dehydrogenation of FA in these experiments. In FA concentrations lower than 0.140 M, the catalytic dehydrogenation of FA appears to be zero order with respect to FA concentration, while at higher FA concentrations one observes half-order dependence (Fig. 8(b)).

Pd_{0.58}Ni_{0.18}Ag_{0.24}/C catalyzed dehydrogenation of FA was also carried out at different [SF]/[FA] ratios by keeping Pd_{0.58}Ni_{0.18}Ag_{0.24}/C and FA concentrations constant and varying SF concentration at 50 °C. The graph of the volume of generated gas (CO₂ + H₂) versus the reaction time for Pd_{0.58}Ni_{0.18}Ag_{0.24}/C catalyzed dehydrogenation of FA at various SF concentrations and 50 °C is depicted in Fig. 9(a). Expectedly, the dehydrogenation rate increases by the increase of SF concentration (or [SF]/[FA] ratio). Plotting the dehydrogenation rate versus SF concentration (both on logarithmic scales) gives a straight line with a slope of 0.48 (Fig. 9(b)). That is an apparent half-order dependence on the SF concentration.

In addition to the effect of catalyst, substrate and promoter concentrations on the dehydrogenation rate, we also investigated the dehydrogenation rate depending on the temperature to find the activation parameters (E_a, ΔH[‡], ΔS[‡]). Pd_{0.58}Ni_{0.18}Ag_{0.24}/C catalyzed dehydrogenation of FA was carried out at different temperatures in the range of 30–70 °C. The volume of generated gas (CO₂ + H₂) versus the reaction time graph for these temperatures is given in Fig. 10(a), which shows the increase in dehydrogenation rate in parallel to temperature increase. The values of observed rate constants *k*_{obs} determined from the nearly linear portions of the volume of generated gas (CO₂ + H₂) versus the reaction time plots at five different temperatures (Fig. 10(a)) are used to plot Arrhenius and Eyring plots (Fig. 10(b–c)) to calculate activation parameters: activation energy E_a = 20.5 kJ/mol, activation enthalpy ΔH[‡] = 17.8 kJ/mol and activation entropy ΔS[‡] = –190 J/mol K (Fig. 10(b–c)). To the best of our knowledge, activation energy value (20.5 kJ/mol) obtained by our Pd_{0.58}Ni_{0.18}Ag_{0.24}/C catalyst is the lowest value ever reported for FA decomposition using a heterogeneous catalyst. The small values of the activation energy and enthalpy and the large negative value of the activation entropy are implying that an associative mechanism occurs in the transition state for Pd_{0.58}Ni_{0.18}Ag_{0.24}/C catalyzed dehydrogenation of FA.

4. Conclusions

In the current work, carbon supported PdNiAg NPs were prepared, characterized and used as heterogeneous catalyst in the dehydrogenation of FA. Some of the major findings of this study can be summarized as follows:

(a) PdNiAg/C was prepared, for the first time, by using a simple and reproducible procedure. The characterization of this new catalytic material by means of ICP-OES, PXRD, XPS, CTEM, HRTEM, STEM, STEM-EDX and HAADF-STEM techniques revealed that

the formation of well-dispersed PdNiAg alloy NPs (5.6 ± 2.2 nm) supported on activated carbon (C).

- (b) The catalytic employment of PdNiAg/C was demonstrated in the dehydrogenation of FA, which has been considered as one of the promising materials for the efficient chemical hydrogen storage. PdNiAg/C catalyst provides high activity (TOF = 85 h^{–1}) and selectivity (~100%) in the dehydrogenation of FA at 50 °C. More importantly, testing the isolability and reusability of PdNiAg/C showed that PdNiAg/C catalyst isolated from the fourth catalytic run still acts as active catalyst in the fifth run of the FA dehydrogenation by retaining >94% of initial activity. ICP-OES and CTEM analyses of the sample harvested from the fifth catalytic run showed that PdNiAg alloy NPs show exceptional stability against to clumping and leaching throughout the catalytic dehydrogenation of FA.
- (c) The quantitative kinetic studies depending on catalyst [PdNiAg], substrate [FA], promoter [SF] concentrations reveal that PdNiAg/C catalyzed dehydrogenation of FA is first-order in catalyst concentration; half-order in promoter concentration and with respect to substrate concentration it appears to be zero when [FA] < 0.140 M and half-order at higher concentrations.
- (d) PdNiAg/C catalyzed dehydrogenation of FA was also investigated by performing this catalytic reaction at different temperatures to evaluate the activation parameters (E_a, ΔH[‡], ΔS[‡]). We found that PdNiAg/C catalyst provides the lowest activation energy (E_a = 20.5 kJ/mol) among the heterogeneous catalysts tested in the same reaction. The activation enthalpy (ΔH[‡] = 17.8 kJ/mol) and activation entropy (ΔS[‡] = –190 J/mol K) values calculated from the Eyring plot are suggestive of the associative mechanism for the PdNiAg/C catalyzed dehydrogenation of FA.

PdNiAg/C as a simple but effective catalyst is believed to strongly encourage the practical applications of FA as a CO-free H₂ generation system for fuel cell applications.

Acknowledgment

The authors thank to Yüzüncü Yıl University (BAP-2013-FEN-B015) for the financial support. MZ thanks to FABED and Science Academy for their financial support to his research.

Appendix A. Supplementary data

Supplementary data associated with this article can be found, in the online version, at <http://dx.doi.org/10.1016/j.apcatb.2014.06.004>.

References

- [1] J. Graetz, Chem. Soc. Rev. 38 (2009) 73–82.
- [2] N.Z. Muradova, T.N. Veziroglu, Int. J. Hyd. Energ. 30 (2005) 225–237.
- [3] J.A. Turner, Science 285 (1999) 687–689.
- [4] L. Schlaphach, A. Zuttel, Nature 414 (2001) 353–358.
- [5] T. Schaub, R.A. Paciello, Angew. Chem. Int. Ed. 50 (2011) 7278.
- [6] D. Preti, C. Resta, S. Squaricalupi, G. Faschinetti, Angew. Chem. Int. Ed. 50 (2011) 12551.
- [7] S. Enthaler, J.V. Langermann, T. Schmidt, Energy Environ. Sci. 3 (2010) 1207–1217.
- [8] M. Yadav, Q. Xu, Energy Environ. Sci. 5 (2012) 9698–9725.
- [9] K.V. Kordesch, G.R. Simader, Chem. Rev. 95 (1995) 191–207.
- [10] T.C. Johnson, D.J. Morris, M. Wills, Chem. Soc. Rev. 39 (2010) 81–88.
- [11] M. Zahmakiran, S. Özkaz, Nanoscale 3 (2011) 3462–3481.
- [12] M. Ojeda, E. Iglesia, Angew. Chem. Int. Ed. 48 (2009) 4800–4803.
- [13] Q.Y. Bi, X.L. Du, Y.M. Liu, Y. Cao, H.Y. He, K.N. Fan, J. Am. Chem. Soc. 134 (2012) 8926–8933.
- [14] X. Gu, Z.-H. Lu, H.-L. Jiang, T. Akita, Q. Xu, J. Am. Chem. Soc. 133 (2011) 11822–11825.
- [15] M. Martis, K. Mori, K. Fujiwara, W.-S. Ahn, H. Yamashita, J. Phys. Chem. C 117 (2013) 22805–22810.

- [16] M. Yadav, A.K. Singh, N. Tsumori, Q. Xu, J. Mater. Chem. 22 (2012) 19146–19150.
- [17] D.A. Bulushev, L. Jia, S. Beloshapkin, J.R.H. Ross, Chem. Commun. 48 (2012) 4184.
- [18] Ö. Metin, X. Sun, S. Sun, Nanoscale 5 (2013) 910–912.
- [19] S. Zhang, Ö. Metin, D. Su, S. Sun, Angew. Chem. Int. Ed. 52 (2013) 3681–3684.
- [20] Y.L. Qin, J. Wang, F.Z. Meng, L.M. Wang, X.B. Zhang, Chem. Commun. 49 (2013) 10028–10030.
- [21] Z.L. Wang, J.M. Yan, H.L. Wang, Y. Ping, Q. Jiang, J. Mater. Chem. A 1 (2013) 12721–12725.
- [22] K. Tedsree, T. Li, S. Jones, C.W.A. Chan, K.M.K. Yu, P.A.J. Bagot, E.A. Marquis, G.D.W. Smith, S.C.E. Tsang, Nat. Nanotech. 6 (2011) 302–307.
- [23] Z.L. Wang, J.M. Yan, Y. Ping, H.L. Wang, W.T. Zheng, Q. Jiang, Angew. Chem. Int. Ed. 52 (2013) 4406–4409.
- [24] R.J. White, R. Luque, V.L. Budarin, J.H. Clark, D.J. Macquarrie, Chem. Soc. Rev. 38 (2009) 481.
- [25] R. Kalimuthu, R.S. Babu, D. Venkataraman, M. Bilal, S. Gurunathan, Coll. Sur. B: Bio. 65 (2008) 150–153.
- [26] S.-H. Wu, D.-H. Chen, J. Coll. Int. Sci. 259 (2003) 282–286.
- [27] R. Ferrando, J. Jellinek, R.L. Johnston, Chem. Rev. 108 (2008) 845–910.
- [28] Y. Zhang, J. Ouyang, H. Yang, Sci. Rep. 3 (3) (2013) 1–6.
- [29] K.-W. Park, J.-H. Choi, B.-K. Kwon, S.-A. Lee, Y.-E. Sung, H.-Y. Ha, S.-A. Hong, H. Kim, A. Wieckowski, J. Phys. Chem. B 106 (2002) 1869–1877.
- [30] P. Prieto, V. Nistor, K. Nouneh, M. Oyama, M.A. Lefdil, R. Diaz, App. Surf. Sci. 258 (2012) 8807.
- [31] H.L. Liu, S. Yoon, S.L. Cooper, G. Cao, J.E. Crow, Phys. Rev. B 60 (1999) 6980–6987.
- [32] Ö. Metin, S. Özkar, S. Sun, J. Am. Chem. Soc. 132 (2010) 1468–1469.
- [33] L. Qi, Y. Gao, J. Ma, Coll. Surf. A: Phys. Eng. Aspects 157 (1999) 285–294.
- [34] X. Huang, H. Zhang, C. Guo, Z. Zhou, N. Zheng, Angew. Chem. 121 (2009) 4902–4906.
- [35] S. Li, Y. Shen, A. Xie, X. Yu, L. Qiu, L. Zhang, Q. Zhang, Green Chem. 9 (2007) 852–858.
- [36] V. Mazumder, M. Chi, K.L. More, S. Sun, Angew. Chem. Int. Ed. 49 (2010) 9368–9371.
- [37] V. Mazumder, M. Chi, K.L. More, S. Sun, J. Am. Chem. Soc. 132 (2010) 7848–7849.
- [38] S. Guo, S. Zhang, D. Su, S. Sun, J. Am. Chem. Soc. 135 (2013) 13879–13884.
- [39] X. Zhou, Y. Huang, W. Xing, C. Liu, J. Liao, T. Lu, Chem. Commun. (2008) 3540–3542.
- [40] Y. Huang, X. Zhou, M. Yin, C. Liu, W. Xing, Chem. Mater. 22 (2010) 5122–5128.
- [41] M. Yadav, T. Akita, N. Tsumori, Q. Xu, J. Mater. Chem. 22 (2012) 12582–12586.
- [42] Y.-L. Qin, J. Wang, F.-Z. Meng, L.-M. Wang, X.-B. Zhang, Chem. Commun. 49 (2013) 10028–10030.
- [43] A. Boddien, F. Gürtner, C. Federsel, P. Sponholz, D. Mellmann, R. Jackstell, H. Junge, M. Beller, Angew. Chem. Int. Ed. 50 (2011) 6411–6414.
- [44] Q.L. Zhu, N. Tsumori, Q. Xu, Chem. Sci. 5 (2014) 195.
- [45] Y.L. Qin, J. Wang, F.Z. Meng, L.M. Wanga, X.-B. Zhang, Chem. Commun. 49 (2013) 10028.